Elementary purinergic Ca^{2+} transients evoked by nerve stimulation in rat urinary bladder smooth muscle

Thomas J. Heppner, Adrian D. Bonev and Mark T. Nelson

Department of Pharmacology, University of Vermont College of Medicine, Burlington, VT 05405-0068, USA

The translation of nerve transmission to Ca^{2+} signals in urinary bladder smooth muscle (UBSM) is incompletely understood. Thus, we sought to characterize Ca^{2+} signals in strips of UBSM loaded with the Ca^{2+}-sensitive fluorescent dye, fluo-4, using laser scanning confocal microscopy. Two types of Ca^{2+} signals occurred spontaneously and could be evoked with field stimulation: large, rapid, global Ca^{2+} transients termed 'global Ca^{2+} flashes', and much smaller, localized Ca^{2+} transients. Global Ca^{2+} flashes were inhibited by the L-type voltage-dependent Ca^{2+} channel (VDCC) inhibitor, diltiazem and with P2X receptor blockade. Simultaneous intracellular recordings and Ca^{2+} measurements indicated that these events are caused by Ca^{2+} influx through VDCCs during action potentials. Small, local Ca^{2+} transients occurred spontaneously, and their frequency could be elevated with field stimulation. Atropine, an inhibitor of muscarinic receptors, did not affect these local Ca^{2+} transients. However, the desensitizing P2X receptor agonist α,β-methylene ATP, and the purinergic antagonist, suramin, effectively inhibited the local Ca^{2+} transients. The frequency of these 'purinergic Ca^{2+} transients' was increased about 7-fold by a 10 s stimulus train (1 Hz). The amplitude, duration at one-half amplitude and the spatial spread of the evoked purinergic Ca^{2+} transients were $F/F_o = 2.4 \pm 0.13$, 111.7 ± 9.3 ms and 14.0 ± 1.0 μm^2, respectively. Tetrodotoxin inhibited evoked purinergic Ca^{2+} transients, indicating that they were dependent on nerve fibre activation. Purinergic Ca^{2+} transients were not dependent on VDCC activity. Neither 2-APB, an inhibitor of inositol 1,4,5-triphosphate ($Ins(1,4,5)P_3$) (IP_3)-induced Ca^{2+} release, nor ryanodine inhibited the purinergic Ca^{2+} transients. We have identified two novel Ca^{2+} signals in rat UBSM. Large, rapid, global Ca^{2+} flashes that represent Ca^{2+} influx through VDCCs during action potentials, and local, purinergic Ca^{2+} transients that represent Ca^{2+} entry through P2X receptors. Our results indicate that purinergic Ca^{2+} transients evoked by release of ATP from nerve varicosities are elementary signals in the process of nerve-smooth muscle communication.

(Resubmitted 20 October 2004; accepted after revision 23 December 2004; first published online 6 January 2005)
Corresponding author T. Heppner: Department of Pharmacology, University of Vermont, Given Building, Rm C-315, 89 Beaumont Avenue, Burlington, VT 05405-0068, USA. Email: thomas.heppner@uvm.edu

The function of the urinary bladder is to relax and store urine during filling, and contract forcefully to empty the bladder during micturition. These seemingly disparate roles are achieved through complex interactions between the autonomic nervous system and urinary bladder smooth muscle (UBSM). UBSM in adult rats is well innervated, receiving approximately 16 000 afferent and efferent axons from ganglion neurones (Gabella, 1999). The bundles of nerve fibres branch repeatedly in UBSM and eventually become single fibres containing varicosities. Located within the varicosities are clear vesicles, or a combination of clear vesicles and dense-cored vesicles (Gabella, 1999) containing neurotransmitters, including acetylcholine (ACh) and ATP or a related purine (Hoyle & Burnstock, 1993; Gabella, 1995). Nerve stimulation evokes the release of ACh and ATP (Dowdall *et al.* 1974; Kasakov & Burnstock, 1982; Theobald & de Groat, 1989; Silinsky & Redman, 1996). ACh binds to muscarinic receptors, stimulating the production of inositol 1,4,5-triphosphate [Ins $(1,4,5)P_3$] (IP_3) and the release of Ca^{2+} from the sarcoplasmic reticulum. ATP binds to, and opens purinergic receptors allowing the influx of cations, including Ca^{2+} and Na^+ (Isenberg *et al.* 1992; Evans *et al.* 1996).

Local Ca^{2+} signals in smooth muscle, in the form of Ca^{2+} waves, were first observed in electrically stimulated rat tail arteries (Iino *et al.* 1994). The release of noradrenaline from surrounding nerve fibres induced Ca^{2+} waves

 DOI: 10.1113/jphysiol.2004.077826

through the activation of (IP_3)-mediated Ca^{2+} release. Stationary, local Ca^{2+} signals (Ca^{2+} sparks), caused by local Ca^{2+} release through a cluster of ryanodine receptors (RyRs), were subsequently detected in smooth muscle (Nelson *et al.* 1995).

Transient increases in Ca^{2+} in smooth muscle have been recorded following the activation of purinerigic receptors. In UBSM, the activation of purinergic receptors induced excitatory junctional potentials (EJPs) and Ca^{2+} transients (Bramich & Brading, 1996; Hashitani *et al.* 2000). Recently, Ca^{2+} imaging techniques revealed fast Ca^{2+} events in smooth muscle following nerve stimulation. Field stimulation of the vas deferens evoked local, transient Ca^{2+} events in smooth muscle cells (neuro-effector Ca^{2+} events). These events were mediated by postsynaptic smooth muscle P2X receptors activated by ATP released at synaptic varicosities (Brain *et al.* 2002, 2003). When the nerve terminals and the neuroeffector Ca^{2+} events were both visualized, it was found that the neuroeffector Ca^{2+} events occurred immediately beneath stimulated sympathetic varicosities. Similar, transient Ca^{2+} events evoked with field stimulation were found in small rat mesenteric arteries and were termed 'junctional Ca^{2+} transients' (Lamont & Wier, 2002; Lamont *et al.* 2003). Line scan images showed that junctional Ca^{2+} transients were evoked immediately following a Ca^{2+} increase in adjacent nerve fibres. Pharmacological studies showed that junctional Ca^{2+} transients were mediated through the activation of purinergic receptors (Lamont & Wier, 2002; Lamont *et al.* 2003).

In the present study, we used a combination of intracellular microelectrode recordings and a laser scanning confocal microscope to image fast Ca^{2+} events in UBSM. Two new Ca^{2+} events whose frequencies are elevated with nerve stimulation, were detected in rat UBSM: (1) large, rapid, global Ca^{2+} flashes that encompass the entire smooth muscle fibre, and are caused by Ca^{2+} influx through L-type voltage-dependent Ca^{2+} channels (VDCCs) during an action potential, and (2) much smaller, localized purinergic Ca^{2+} transients. Although similar in appearance to RyR-mediated Ca^{2+} sparks (Nelson *et al.* 1995; Herrera *et al.* 2001; Heppner *et al.* 2003), these purinergic Ca^{2+} transients are larger and longer than Ca^{2+} sparks and represent a novel elementary Ca^{2+} signal mediated by the activation of P2X receptors. Purinergic Ca^{2+} transients probably play a critical, initial role in nerve-evoked excitation–contraction coupling in UBSM.

Methods

Tissue preparation

Adult male rats were killed by pentobarbital sodium (130 mg (kg body weight)$^{-1}$), followed by thoracotomy in accordance with the guidelines for the use and care of laboratory animals (NIH publication 85-23, 1985) and as approved by the Institutional Animal Use and Care Committee of the University of Vermont. The urinary bladder was quickly removed and placed in cold Hepes-buffered saline. Strips of UBSM (approximately 0.5 mm thick × 1 mm wide × 5 mm long) were carefully removed from the serosal surface with sharp scissors and pinned to small sylgard blocks. The sylgard blocks with the attached UBSM strips were placed tissue side down, in a chamber specially designed to measure rapid Ca^{2+} responses. To allow fresh physiological saline solution (PSS) to flow under and around the tissue strip, thin spacers (0.2 mm) were placed on either side of the tissue. The tissue was superfused (1–2 ml min^{-1}) with a PSS at 37°C. For the experiments quantifying the small, localized Ca^{2+} transients, sucrose (12%) was added to the superfusing PSS to reduce tissue movement (Foster *et al.* 1989; Heppner *et al.* 1997). Sucrose was not added to the PSS in the simultaneous measurement of Ca^{2+} and membrane potential with microelectrodes, or in experiments involving the large, rapid global Ca^{2+} events. Drugs were dissolved in the superfusing salt solution and applied for at least 20 min prior to image acquisition unless otherwise indicated.

Ca^{2+} imaging and analysis

Strips of UBSM were imaged with a laser scanning confocal microscope (OZ; Noran Instruments) attached to a Nikon diaphot microscope. A Nikon ×60 water immersion objective (NA 1.2) was used to visualize the tissue. Images were acquired using an Intervision software package controlled by a Silicon graphics Workstation (O_2). To visualize Ca^{2+} events in UBSM, the tissue was placed in a Hepes solution containing the Ca^{2+} fluorescent dye, fluo-4 AM (10 μM) (Molecular Probes; Eugene, OR, USA) and pluronic acid (2.5 μg ml^{-1}; Molecular Probes). To facilitate loading of the dye, the tissue was kept in the dark for 60 min at 21–23°C followed by a wash in normal Hepes buffer (21–23°C) before placing the tissue in PSS. All experiments were conducted in PSS (37°C). A krypton–argon laser was used to excite fluo-4 and the emitted light was captured at wavelengths >500 nm. For most experiments, images were acquired at 30 images s^{-1} (every 33.33 ms). The size of the field was 116 × 109 μm (512 × 480 pixels). To measure latency, images were acquired at 240 images s^{-1}, an acquisition rate that yields an interimage interval of 4.13 ms. Image analysis was conducted offline using customized software written in our laboratory (Dr Adrian Bonev). Evoked Ca^{2+} transients were detected by measuring an increase in the fractional fluorescence of Ca^{2+} $F/F_o = 1.3$, that could be distinguished above the background noise. Baseline fluorescence was measured by averaging at least 10 images

with no Ca^{2+} transients. Ca^{2+} transients were measured using a $1.5 \times 1.5\ \mu$m box (7×7 pixels) and analysed as previously described (Perez *et al.* 1999; Jaggar & Nelson, 2000; Wellman *et al.* 2001) using customized software written in our laboratory.

Field stimulation

The nerves in the strip were excited with platinum electrodes placed in the recording chamber, which were attached to the output of the stimulus isolation unit of a Grass S44 stimulator. Voltages used to evoke Ca^{2+} transients ranged from 30 to 100 V. A frequency of 1 Hz and a pulse duration of 0.2 ms was used throughout this study. Ca^{2+} transients were evoked with a train of stimuli applied for 10 s at a frequency of 1 Hz. This relatively low frequency allowed individual Ca^{2+} events to be identified, and facilitated quantification of these events during the stimulus train. Global Ca^{2+} events were evoked by increasing the stimulating voltage until threshold was reached. The smaller evoked Ca^{2+} transients were visualized by reducing the stimulating voltage just below threshold for the global Ca^{2+} events.

Microelectrode intracellular recording

To record voltage from UBSM cells, strips of tissue were prepared as above for Ca^{2+} imaging. Standard microelectrode techniques were used. Oxygenated PSS was superfused over the tissue strips at 1–2 ml min^{-1} (37°C). Microelectrodes were pulled on a Flaming/Brown gas puller (Sutter Instruments, Novato, CA, USA) and had resistances of 60–80 MΩ when filled with 2.0 M KCl. The transmembrane potential was acquired using an Axoclamp 2A (Axon Instruments, Union City, CA, USA) and recorded using Axotape software (Axon Instruments). The membrane potential was measured as the difference between the reference electrode in the bath and the intracellular microelectrode.

Experimental design

Each experiment consisted of three to five 15 s recordings from the same field during which a 10 s stimulus train (1 Hz) was applied. One to three files were recorded under control conditions and after drug application. The time interval between each file was at least 5 min. The tissue was incubated for at least 20 min in drug-containing solutions before test stimuli were applied.

Drugs and solutions

UBSM strips were removed from the urinary bladder in Hepes solution with the following composition (mM): NaCl, 134; KCl, 6; $MgCl_2$, 1; $CaCl_2$, 2; Hepes, 10; glucose, 10; (pH 7.4). NaOH was used to adjust the pH of Hepes solutions. Evoked Ca^{2+} transients were measured in PSS with the following composition (mM): NaCl, 119; KCl, 4.7; $NaHCO_3$, 23.8; KH_2PO_4, 1.2; $CaCl_2$, 1.6; $MgCl_2$, 1.2, EDTA, 0.023; and glucose, 11.0 (pH 7.4). PSS was continuously bubbled with 95% O_2–5% CO_2. For experiments using nominal Ca^{2+}-free solution, Ca^{2+} was omitted from the superfusing PSS. 2-Aminethoxydiphenyl-borate (2-APB) was obtained from Tocris (Ellisville, MO, USA), ryanodine was obtained from LC laboratories (Woburn, MA, USA) and diltiazem, α,β-methylene ATP, suramin, atropine, and tetrodotoxin (TTX) were obtained from Sigma (St Louis, MO, USA).

Statistics

Data were normalized to control, and expressed as mean ± S.E.M. At least three paired experiments were conducted for each paradigm using at least three rats. n refers to the number of evoked Ca^{2+} transients or the number of preparations as indicated in the text. To determine significance, Ca^{2+} events under control conditions were compared to Ca^{2+} events following drug treatment using a paired student's t test on the raw data. Significance was determined at $P \leq 0.05$.

Results

Rapid, global Ca^{2+} events in UBSM are caused by Ca^{2+} influx during an action potential

UBSM strips, loaded with fluo-4, appeared as dark grey, homogenous bundles when examined with a laser scanning confocal microscope. In a single field, several bundles of UBSM were often seen lying in parallel. Alongside and between the bundles of smooth muscle were thin, very bright fibres that usually ran in parallel with the smooth muscle bundles. Based on their location and morphology, these fibres were probably nerve processes innervating the smooth muscle (Gabella, 1995; Gabella & Davis, 1998; Drake *et al.* 2003).

In PSS, smooth muscle bundles displayed repetitive, large, very rapid increases in Ca^{2+} that spread quickly along the length of the bundle. These Ca^{2+} events occurred spontaneously or could be evoked with field stimulation. We termed these large, rapid, global Ca^{2+} events 'global Ca^{2+} flashes'. These events were sensitive to P2X receptor inhibition. Treatment with α,β-methylene ATP (10 μM), a P2X receptor agonist, which desensitizes P2X receptors, and suramin (10 μM), an inhibitor of P2X receptors, significantly decreased the number of spontaneous global Ca^{2+} flashes to 20.0 ± 13.0% of control ($n = 6$ preparations; $P < 0.05$) and also significantly decreased the number of global Ca^{2+} flashes evoked by stimulation to 36.3 ± 12.0% of control ($n = 8$ preparations; $P < 0.05$).

This suggests that P2X receptor activation contributes to spontaneous and evoked global Ca^{2+} transients.

To identify the origin of the global Ca^{2+} flashes, a single muscle bundle was impaled with a microelectrode to record changes in the membrane potential. Simultaneous recordings of Ca^{2+}-activated fluorescence changes and membrane potential showed that each global Ca^{2+} flash was evoked by a single action potential (Fig. 1). Since the upstroke of the action potential is dependent on Ca^{2+} influx through VDCCs, the global Ca^{2+} flash should be reduced when these channels are blocked. Diltiazem, a reversible inhibitor of VDCCs, markedly decreased these events (Fig. 2). For example, in one preparation, 68 global Ca^{2+} flashes were recorded in PSS during a 15 s recording using 1 Hz stimulation. Diltiazem (100 μM; 20 min) eliminated these events. Following a 35 min rinse in PSS, 70 global Ca^{2+} flashes were recorded. Simultaneous recordings of Ca^{2+} fluorescence and membrane potential from bundles of UBSM, along with the sensitivity of the global Ca^{2+} flashes to an inhibitor of VDCCs indicate that each global Ca^{2+} flash results from Ca^{2+} influx during an action potential. Immediately following the global Ca^{2+} flashes, the UBSM would contract suggesting that the VDCC-mediated Ca^{2+} influx is causally related to UBSM contraction.

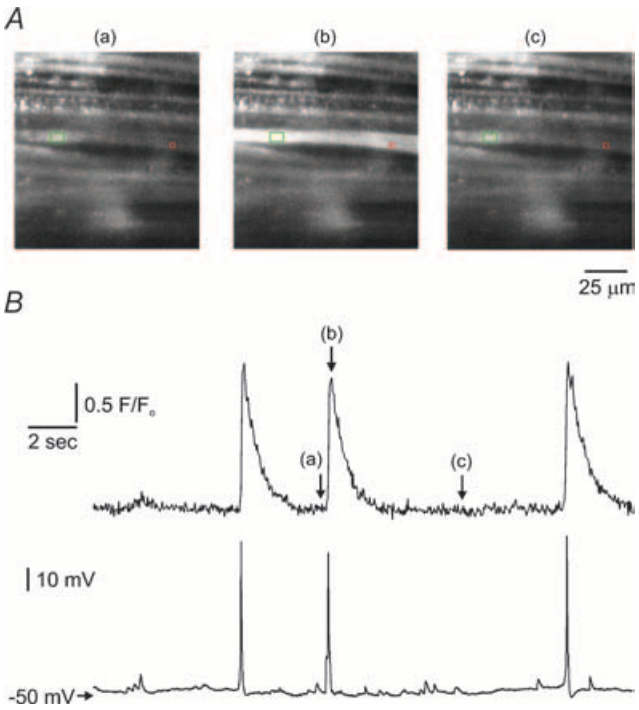

Figure 1. Simultaneous recording of Ca^{2+} and voltage from a single bundle of UBSM
A, images recorded from UBSM in normal PSS (37°C) loaded with fluo-4. The muscle bundles are orientated horizontally. Images were acquired at 30 images s^{-1}. The letters above each image correspond to changes in Ca^{2+}-activated fluorescence in *B* (upper trace) and were recorded before (*a*), during (*b*) and after (*c*) a spontaneous action potential in the UBSM bundle impaled with the microelectrode. *B*, simultaneous recordings of changes in Ca^{2+}-activated fluorescence (upper trace) and voltage (lower trace) from a single bundle of UBSM. Changes in Ca^{2+}-activated fluorescence were measured from the red box in *A* located on the impaled muscle bundle. The microelectrode impalement site is indicated by the green rectangle. Notice that each of the three action potentials induced a simultaneous increase in the Ca^{2+}-activated fluorescence. The large increase in Ca^{2+}-activated fluorescence from a single muscle bundle during an action potential is also shown above in *Ab*.

Nerve stimulation elevates the frequency of local Ca^{2+} transients

In addition to the global Ca^{2+} flashes, smaller, more localized Ca^{2+} transients were also evident in UBSM. These localized Ca^{2+} transients became more apparent when the global Ca^{2+} flashes were inhibited with either VDCC blockers or when sucrose (12%) was added to the superfusing PSS to restrict tissue movement. The frequency of these small Ca^{2+} transients could be elevated by low-frequency field stimulation (1 Hz) (Fig. 3) (movie file provided as supplemental data). To evoke these small Ca^{2+} transients with field stimulation, the stimulating voltage was decreased to a level just below the threshold needed to induce global Ca^{2+} flashes. To measure the effect of field stimulation on the frequency of these events, Ca^{2+} transients were recorded from the same field before and after stimulation (10 s at 1 Hz). Nerve stimulation significantly elevated the frequency of the Ca^{2+} transients about 7-fold, from 23 ± 8.4 to 156 ± 35.9 events ($P < 0.05$; $n = 4$ preparations).

Purinergic receptor, but not muscarinic receptor, activation mediates the localized Ca^{2+} transients

Parasympathetic nerve fibres innervating UBSM corelease ACh and ATP in response to nerve stimulation (Kasakov & Burnstock, 1982; Theobald & de Groat, 1989). Activation of muscarinic receptors induces IP_3-mediated release of Ca^{2+} from internal stores. ATP activates P2X receptor channels which permit the influx of Na^+ and Ca^{2+} ions into UBSM cells. To study the link between nerve transmission and evoked Ca^{2+} transients, we used selective pharmacological inhibitors of muscarinic and purinergic receptors. Atropine (10 μM), which inhibits muscarinic receptors, did not significantly affect the frequency of evoked local Ca^{2+} transients (Fig. 4). To assess the contribution of P2X receptors to the evoked Ca^{2+} transients, we used compounds that inhibit P2X receptor function. Suramin (10 μM) and α,β-methylene ATP (10 μM) nearly abolished the local Ca^{2+} transients evoked with field stimulation (Fig. 4). In addition, P2X receptor inhibition significantly decreased the number of spontaneous Ca^{2+} transients to $19.0 \pm 7.0\%$ of control (20 s file; α,β-methylene ATP, 10 μM and suramin, 10 μM)

($P < 0.05$; $n = 4$ preparations). These results indicate that the majority of spontaneous Ca^{2+} transients and evoked Ca^{2+} transients are purinergic in nature and probably reflect the influx of Ca^{2+} into UBSM through P2X receptors. We refer to these events as 'purinergic Ca^{2+} transients' hereafter.

Latency of purinergic Ca^{2+} transients from onset of nerve stimulation

To explore the relationship between nerve stimulation and purinergic Ca^{2+} transients, the time between nerve stimulation and the appearance of the local Ca^{2+} event (latency) was determined by acquiring images at the rate of 240 images s^{-1}. At this acquisition rate, the time interval between images was 4.13 ms. Figure 5*A* and *B* shows the onset and decay of two Ca^{2+} events following a single stimulus. The purinergic Ca^{2+} transients occurred as early as 8 ms after a stimulus, with most Ca^{2+} events occurring 12–16 ms following a stimulus (Fig. 5*C*). These purinergic Ca^{2+} transients often appeared to originate from nerve fibres, and occurred repeatedly from the same site.

TTX inhibits purinergic Ca^{2+} transients evoked with field stimulation

Since both UBSM and nerve fibres could potentially be activated by field stimulation, a pulse duration of 0.2 ms was used to selectively activate nerve fibres (Hashitani *et al.* 2000; Herrera *et al.* 2000). However, to ensure that the purinergic Ca^{2+} transients were not caused by direct activation of UBSM, tetrodotoxin (TTX) 2 μM was added to the superfusing solution to inhibit voltage-gated Na^{+} channels located on nerve processes. In paired experiments, the number of spontaneous purinergic Ca^{2+} transients recorded during 20 s files was not significantly affected by TTX (2 μM) (TTX 109.0 ± 24.0% of control, $n = 4$ preparations). In contrast, TTX (2 μM), significantly decreased the frequency of evoked purinergic Ca^{2+} transients (TTX 17.0 ± 8.0% of control, $P < 0.05$, $n = 4$

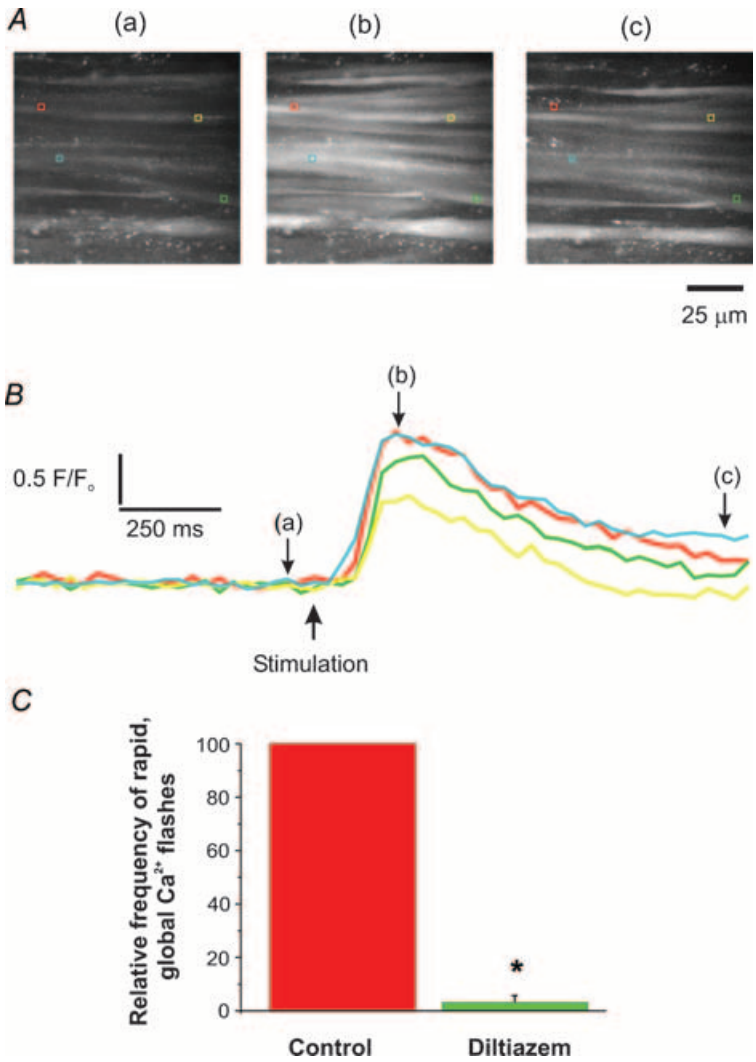

Figure 2. Global Ca^{2+} flashes in UBSM recorded during field stimulation
A, average images (acquired at 30 images s^{-1}) showing bundles of smooth muscle before (*a*), approximately 100 ms following a single stimulus pulse (*b*), and approximately 1 s following field stimulation (*c*). Several bundles demonstrated an increase in Ca^{2+}-activated fluorescence changes following stimulation. *B*, the changes in Ca^{2+}-activated fluorescence were recorded from the regions of interest (coloured boxes) in *A* showing a rapid increase in Ca^{2+}-activated fluorescence and a slow return to resting Ca^{2+} levels following field stimulation. Letters *a*, *b* and *c* correspond to the images in *A*. *C*, the relative number of global Ca^{2+} flashes from paired experiments recorded during field stimulation in control and with diltiazem (100 μM). Inhibition of VDCCs significantly decreased the number of these global Ca^{2+} flashes. $^{*}P < 0.05$, $n = 3$ preparations.

preparations), indicating that evoked purinergic Ca^{2+} transients were dependent on the activation of nerve fibres.

Purinergic Ca^{2+} transients do not depend on Ca^{2+} influx through VDCCs

The opening of VDCCs allows Ca^{2+} influx into UBSM. It is possible that localized Ca^{2+} entry through VDCCs into UBSM contributes to purinergic Ca^{2+} transients. To examine this possibility, we applied the VDCC inhibitor, diltiazem (100 μM), before field stimulation (1 Hz). Inhibiting VDCCs did not significantly reduce the frequency (diltiazem, $87.0 \pm 7.0\%$ of control, $n = 3$ preparations) or amplitude (control, 2.0 ± 0.04 F/F_0, $n = 246$ Ca^{2+} events; diltiazem, 2.0 ± 0.03 F/F_0, $n = 310$ Ca^{2+} events) of the purinergic Ca^{2+} transients, indicating that Ca^{2+} influx through VDCCs does not contribute to purinergic Ca^{2+} transients.

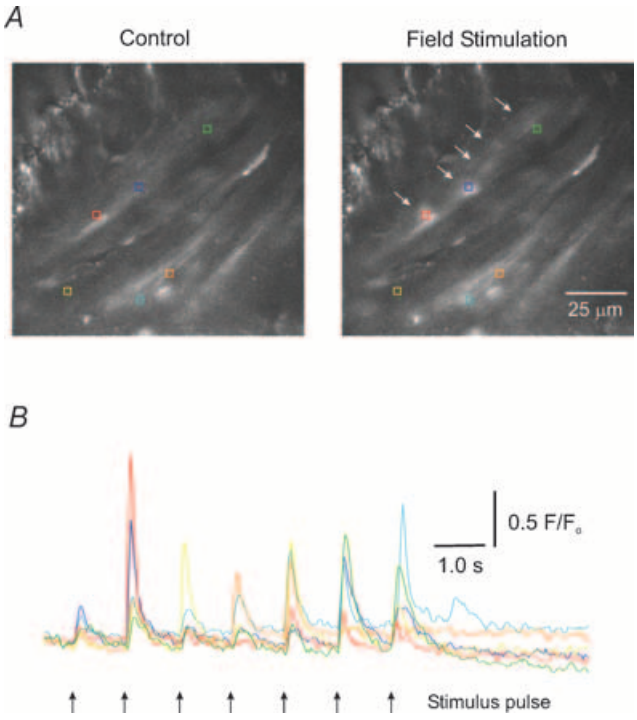

Figure 3. Local Ca^{2+} responses in UBSM evoked with field stimulation
A, images of UBSM show smooth muscle (acquired at 30 images s^{-1}) bundles running diagonally from the lower left to the upper right of each image before (left panel) and after (right panel) a single stimulus pulse. Coloured boxes enclose regions of interest where evoked Ca^{2+} responses occur, and correspond to the coloured traces below in *B*. The white arrows in the right panel show Ca^{2+} responses occurring in response to a single stimulus and correspond to the second stimulus pulse from the left in *B*. *B*, changes in Ca^{2+}-activated fluorescence in response to seven stimulus pulses (1 Hz). Note that with each pulse a Ca^{2+} transient occurs in some of the selected regions of interest (movie file provided as supplemental data).

P2X receptor channels are permeable to both Ca^{2+} and Na^{+} ions. Therefore, purinergic Ca^{2+} transients should depend on external Ca^{2+}. Removing external Ca^{2+} significantly decreased the frequency of purinergic Ca^{2+} transients. In the absence of stimulation, the frequency of spontaneous purinergic Ca^{2+} transients was significantly decreased in Ca^{2+}-free external solution to $14.0 \pm 9.0\%$ of control ($n = 4$ preparations; $P < 0.05$). Returning Ca^{2+} to the external solution increased the frequency of purinergic Ca^{2+} transients to control levels ($106.0 \pm 17.0\%$ of control, $n = 4$ preparations). The frequency of evoked purinergic Ca^{2+} transients was also inhibted significantly in Ca^{2+}-free solution to $15.0 \pm 5.0\%$ of control ($n = 4$ preparations). When Ca^{2+} was returned to the external solution, the frequency of evoked purinergic Ca^{2+} transients returned to $77.0 \pm 10.0\%$ of control. Although it is likely that the release of transmitter from nerve terminals would also be blocked, these findings indicate that purinergic Ca^{2+} transients are dependent on external Ca^{2+} and suggest that internal Ca^{2+} release does not underlie these events.

Ca^{2+} release through IP_3 receptors and RyRs does not contribute to the purinergic Ca^{2+} transients

In smooth muscle, IP_3-mediated Ca^{2+} release produces Ca^{2+} waves (Iino *et al.* 1993), and Ca^{2+} release through RyRs can produce Ca^{2+} sparks which activate large-conductance potassium channels and lead to membrane hyperpolarization (Nelson *et al.* 1995; Jaggar *et al.* 2000; Herrera *et al.* 2001; Heppner *et al.* 2003). To study the contribution of Ca^{2+} release from internal stores to purinergic Ca^{2+} transients, we examined

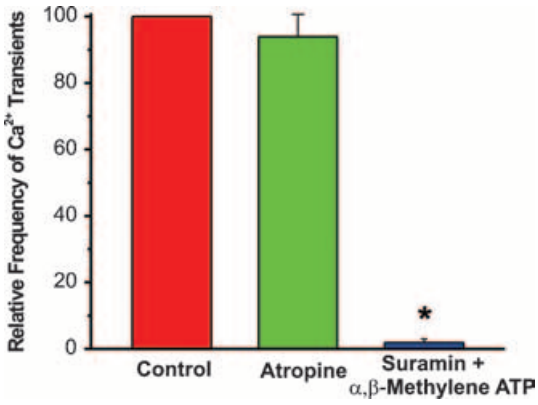

Figure 4. Inhibition of P2X receptors, but not muscarinic receptors, significantly decreased the frequency of evoked Ca^{2+} transients
Column graph showing no change in evoked Ca^{2+} transients with muscarinic receptor inhibition by atropine (10 μM), but nearly complete abolition of these events when P2X receptors are blocked with suramin (10 μM) and α,β-methylene ATP (10 μM). To account for the variability in the number of events between different preparations, the data were normalized to control. $^*P < 0.05$, $n = 3$ preparations.

purinergic Ca^{2+} transients following inhibition of IP_3 receptors with 2-APB (100 μM), and inhibition of RyRs with ryanodine (10 μM). The inhibition of IP_3 receptors did not significantly alter the frequency (2-APB, 81.0 ± 10.0% of control, $n = 4$ preparations) or amplitude (control, 2.0 ± 0.02 F/F_0, $n = 711$ purinergic Ca^{2+} transients; 2-APB, 2.0 ± 0.02 F/F_0, $n = 541$ purinergic Ca^{2+} transients) of purinergic Ca^{2+} transients. Similarly, the inhibition of RyRs did not significantly alter the frequency (ryanodine 106.0 ± 10.0% normalized to control, $n = 4$ preparations) or amplitude of purinergic Ca^{2+} transients (control, 1.9 ± 0.18 F/F_0, $n = 339$ purinergic Ca^{2+} transients; ryanodine, 1.9 ± 0.18 F/F_0, $n = 639$ purinergic Ca^{2+} transients). These findings suggest that Ca^{2+} release from internal stores does not significantly contribute to purinergic Ca^{2+} transients.

Ca^{2+} sparks and purinergic Ca^{2+} transients represent two discrete elementary Ca^{2+} events in UBSM

Ca^{2+} sparks are localized, transient events mediated by the release of sarcoplasmic reticulum Ca^{2+} through RyRs in smooth muscle (Nelson *et al.* 1995; Jaggar *et al.* 2000), including UBSM (Imaizumi *et al.* 1999; Kotlikoff *et al.* 1999; Herrera *et al.* 2001; Ohi *et al.* 2001). Purinergic Ca^{2+} transients are also brief, localized Ca^{2+} events, but represent Ca^{2+} influx through purinergic receptors. In the presence of ryanodine (10 μM), which blocks Ca^{2+} sparks, a population of larger events remained that were evoked by field stimulation. These events were sensitive to the purinergic receptor inhibitors, α,β-methylene ATP (10 μM) and suramin (10 μM). Inhibition of purinergic receptors left a population of Ca^{2+} events that were smaller in amplitude and frequency (Ca^{2+} sparks). When the kinetics of each type of elementary Ca^{2+} transient were measured, we found that the purinergic Ca^{2+} transients were larger in amplitude, duration and spread compared to Ca^{2+} sparks (Fig. 6).

Discussion

In this study, we identified three different Ca^{2+} signals in UBSM: (1) global Ca^{2+} flashes, which are large, rapid Ca^{2+} signals that arise from Ca^{2+} influx through VDCCs during an action potential, last for several seconds, and occupy the entire smooth muscle cell; (2) purinergic Ca^{2+} transients, which are smaller, local Ca^{2+} transients in UBSM mediated by Ca^{2+} influx through purinergic receptor channels; (3) Ca^{2+} sparks, which are localized Ca^{2+} events mediated by Ca^{2+} release through RyRs.

Global Ca^{2+} flashes represent Ca^{2+} influx during action potentials

Global Ca^{2+} flashes in UBSM occurred spontaneously, were evoked with field stimulation, and were sensitive to the inhibition of P2X receptors. These events travelled along the length of the UBSM bundle and were immediately followed by tissue contraction. These events were dependent on the influx of Ca^{2+} through VDCCs, since they were substantially reduced by the VDCC

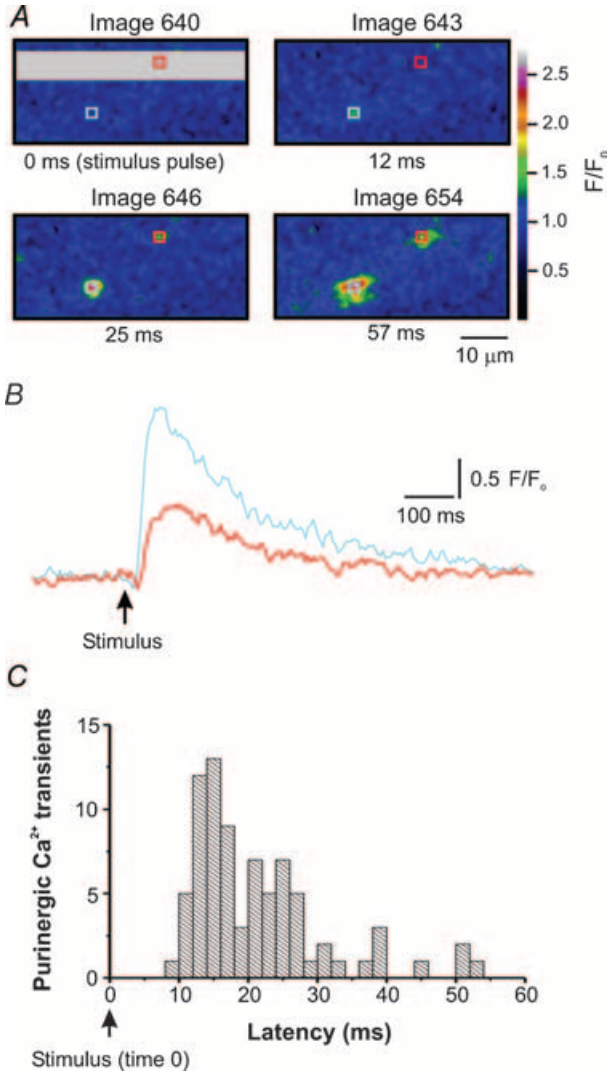

Figure 5. Field stimulation (1 Hz) evokes purinergic Ca^{2+} transients in UBSM
A, four panels showing the stimulus flash followed by the onset of purinergic Ca^{2+} transients. The beginning of the grey region (upper left corner of grey area) of the upper left panel shows the precise time the stimulus was delivered to the tissue. About 12 ms following the stimulus (upper right panel), a purinergic Ca^{2+} transient appears in the light blue region of interest, followed 25 ms after the stimulus by a second purinergic Ca^{2+} transient in the red region of interest (lower left panel). The lower right panel shows the purinergic Ca^{2+} transients near their peak. *B*, the changes in Ca^{2+}-activated fluorescence from the regions of interest in *A* before and after a stimulus pulse. Notice the rapid onset and slow decay of these purinergic Ca^{2+} transients. *C*, the latency of purinergic Ca^{2+} transients is displayed graphically. The earliest purinergic Ca^{2+} transients were recorded about 8 ms after the stimulus and reached a peak between 12 and 16 ms after stimulation.

blocker, diltiazem (see Figs 1 and 2). This view is supported by the finding that the upstroke of the action potential is mediated by Ca^{2+} influx through VDCCs (Klockner & Isenberg, 1985; Mostwin, 1986; Heppner *et al.* 1997; Hashitani *et al.* 2000; Hashitani & Brading, 2003*a*,*b*) and is consistent with the observation that action potentials occur spontaneously in UBSM (Creed *et al.* 1983; Heppner *et al.* 1997; Hashitani *et al.* 2000, 2001; Hashitani & Brading, 2003*a*,*b*). Simultaneous recordings of voltage and Ca^{2+} in the guinea-pig UBSM revealed a Ca^{2+} transient associated with each action potential similar to the findings of the present study (Hashitani *et al.* 2001, 2004*a*,*b*). The block of Ca^{2+} global flashes by purinergic receptor inhibitors indicates that the activation of purinergic receptors is involved in the generation of VDCC-dependent action potentials and global Ca^{2+} flashes.

Nerve stimulation evokes purinergic Ca^{2+} transients

The frequency of purinergic Ca^{2+} transients increased with field stimulation when the pulse duration was selective for nerve fibres. When conduction along nerve fibres was blocked by inhibiting voltage-gated Na^+ channels with TTX, evoked purinergic Ca^{2+} transients were not detected. These results indicate that the activation of nerve fibres in the UBSM significantly elevates the frequency of purinergic Ca^{2+} transients.

A property of synaptic transmission is latency, or the brief delay between presynaptic cell stimulation and the response in the postsynaptic cell. The latency of purinergic Ca^{2+} transients recorded with line scan confocal imaging was <3 ms in mesenteric arteries (Lamont & Wier, 2002), and about 6 ms in the vas deferens (Brain *et al.* 2002). Using high-speed confocal imaging (240 images s^{-1}), events could be detected as soon as 8 ms following the stimulus, with the peak latency of purinergic Ca^{2+} transients in UBSM at 12–16 ms. There was approximately 4.1 ms between images at an acquisition rate of 240 images s^{-1}, and therefore, the maximum error in latency would be 4.1 ms. Therefore, the latency of purinergic Ca^{2+} transients in UBSM was consistent with the delay found in other smooth muscle tissues. This result, in conjunction with the inhibitory effect of TTX, indicates that purinergic Ca^{2+} transients result from nerve fibre stimulation and synaptic transmission, and not direct stimulation of UBSM.

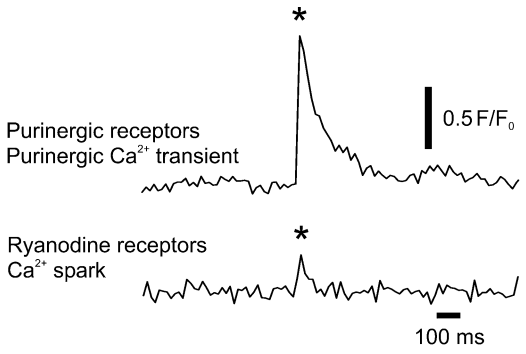

	Purinergic Ca^{2+} transient	RyR Ca^{2+} spark
F/F_0	2.4 ± 0.13*	1.5 ± 0.03
t one/half (ms)	111.7 ± 9.3*	33.6 ± 4.5
Spread μ^2	14.0 ± 1.0*	4.8 ± 0.5

Figure 6. Ca^{2+}-activated fluorescence for purinergic Ca^{2+} transients and Ca^{2+} sparks in UBSM
The upper trace represents a purinergic Ca^{2+} transient (*) through P2X receptors recorded in the presence of ryanodine (10 μM) to inhibit Ca^{2+} sparks. The lower trace represents a Ca^{2+} spark (*) recorded in the presence of suramin (10 μM) and α,β-methylene ATP (10 μM) to block P2X receptors. Kinetic data from these traces show that purinergic Ca^{2+} transients mediated through P2X receptors are larger in amplitude and duration than Ca^{2+} sparks. In the table * indicates a significant difference ($P < 0.05$) between purinergic Ca^{2+} transients and RyR Ca^{2+} sparks.

External Ca^{2+}, but not VDCCs, is necessary to evoke purinergic Ca^{2+} transients

The purinergic Ca^{2+} transients should be dependent on external Ca^{2+}, since P2X receptors are highly permeable to Ca^{2+}. Removing Ca^{2+} from the external solution significantly decreased the frequency of purinergic Ca^{2+} transients. This effect was largely reversible, since the frequency of purinergic Ca^{2+} transients increased with the re-introduction of Ca^{2+} to the external medium. The removal of external Ca^{2+} could also inhibit the release of ATP from nerve terminals and thereby decrease purinergic Ca^{2+} transients. Our experiments do not differentiate between these two possibilities. However, if the removal of external Ca^{2+} had no effect on purinergic Ca^{2+} transients, then this would argue against Ca^{2+} influx through P2X receptor channels.

Another possibility is that Ca^{2+} influx through VDCCs contributes to the purinergic Ca^{2+} transients. VDCCs in UBSM (Creed *et al.* 1983; Heppner *et al.* 1997; Herrera *et al.* 2001; Herrera & Nelson, 2002; Hashitani & Brading, 2003*a*,*b*) are voltage sensitive and play a key role in mediating Ca^{2+} entry into UBSM cells, such as would occur during an action potential (Klockner & Isenberg, 1985; Mostwin, 1986; Heppner *et al.* 1997; Hashitani & Brading, 2003*b*). However, Ca^{2+} influx through VDCCs does not appear to contribute to purinergic Ca^{2+} transients for several reasons: (1) the duration of our stimulating pulse (0.2 ms) is selective for nerve fibres, and not likely to depolarize UBSM; (2) inhibition of VDCCs

with diltiazem did not significantly decrease the frequency of purinergic Ca^{2+} transients; (3) the spatial spread of Ca^{2+} was local, and did not include the entire cell as would be expected with VDCC activation. Therefore, in this study, diltiazem-sensitive VDCCs do not appear to contribute to the purinergic Ca^{2+} transients.

Purinergic Ca^{2+} transients do not require Ca^{2+}release from internal stores

Ca^{2+} stores in the sarcoplasmic reticulum are critical to many cellular functions and underlie Ca^{2+} transient events such as Ca^{2+} sparks and Ca^{2+} waves. Ca^{2+} sparks are generated by the release of Ca^{2+} through RyRs located on the sarcoplasmic reticulum (Nelson *et al.* 1995; Herrera *et al.* 2001; Heppner *et al.* 2003). Ca^{2+} waves are generated by the activation of IP_3 receptors (Iino *et al.* 1993). Activation of muscarinic receptors leads to the production of IP_3. Both M2 and M3 receptor subtypes are found in the urinary bladder. The M3 receptor is coupled to the Gq family of proteins and generates the production of IP_3 and internal Ca^{2+} release (Caulfield, 1993). The M3 subtype mediates contraction in the urinary bladder (Hegde & Eglen, 1999) and could trigger the release of Ca^{2+} from the sarcoplasmic reticulum. However, the frequency of purinergic Ca^{2+} transients was not reduced when muscarinic receptors were blocked with atropine, suggesting that muscarinic receptor activation does not contribute to the initiation of the purinergic Ca^{2+} transients in UBSM.

Inhibition of Ca^{2+} release through RyRs (ryanodine, 10 μM) or through IP_3 receptors (2-APB, 100 μM) and block of the production of IP_3 by inhibition of the muscarinic receptor (atropine, 10 μM) did not alter the frequency of purinergic Ca^{2+} transients in UBSM. Similar results were also observed in arteries. Gitterman & Evans (2001) found that Ca^{2+}-induced Ca^{2+} release was not involved in P2X-receptor-mediated contractions in rat mesenteric arteries, but that all the Ca^{2+} for contraction enters through P2X receptors. Therefore, in UBSM the release of Ca^{2+} from internal stores is not crucial to the generation of the purinergic Ca^{2+} transients.

Purinergic Ca^{2+} transients are mediated through purinergic receptors

P2X receptors belong to a family of ATP-sensitive ligand-gated cation channels ($P2X_1$–$P2X_7$) formed by the assembly of 3–6 individual subunits (Khakh *et al.* 2001). In the cat UBSM, the $P2X_2$ receptor is the predominant subtype followed by the $P2X_1$ receptor (Birder *et al.* 2004). However, in rodents the homomeric $P2X_1$ receptor subtype is clearly associated with the membranes of UBSM (Lee *et al.* 2000; Elneil *et al.* 2001; Vial & Evans, 2000) and underlies the P2X receptor activity in UBSM as demonstrated in $P2X_1$ receptor-deficient mice (Vial & Evans, 2000). Although some studies found no evidence of $P2X_1$ clustering in rat or human urinary bladders (Elneil *et al.* 2001), other studies employing rat urinary bladder demonstrated $P2X_1$ receptors distributed in clusters on smooth muscle membranes adjacent to nerve varicosities (Hansen *et al.* 1998; Dutton *et al.* 1999; Yunaev *et al.* 2000). These studies provide anatomical evidence of nerve fibre varicosities and $P2X_1$ receptors, possibly in clusters, adjacent to one another.

Activation of P2X receptors allows the influx of cations, including Ca^{2+} and Na^+ ions, into the cell. Recent Ca^{2+} imaging studies identified ATP-evoked Ca^{2+} events in the vas deferens (Brain *et al.* 2002, 2003) and in mesenteric arterial smooth muscle (Lamont & Wier, 2002; Lamont *et al.* 2003). In the vas deferens, stimulation of sympathetic fibres released ATP that activated P2X receptors. The Ca^{2+} influx through the P2X receptor was termed 'neuroeffector Ca^{2+} transients' (Brain *et al.* 2002, 2003). Similarly, in mesenteric artery smooth muscle, Ca^{2+} transients, termed 'junctional Ca^{2+} transients' were evoked by the activation of P2X receptors located on the smooth muscle, by ATP released from sympathetic fibres. This influx of Ca^{2+} through the P2X receptors in mesenteric arteries comprises the junctional Ca^{2+} transient (Lamont & Wier, 2002; Lamont *et al.* 2003). The kinetics of these Ca^{2+} events are similar to the evoked purinergic Ca^{2+} transients presently described in UBSM. Since evoked Ca^{2+} transients are blocked by inhibitors of P2X receptors, it is likely that the activation of a cluster of $P2X_1$ receptors by nerve-evoked release of ATP underlies the evoked Ca^{2+} transients observed in the present study (Fig. 7). In UBSM, voltage recordings revealed excitatory junction potentials (EJPs), which are brief membrane potential depolarizations mediated by P2X receptors. EJPs initiate action potentials in UBSM, transient increases in Ca^{2+} that are followed by contractions (Bramich & Brading, 1996; Hashitani *et al.* 2000). Since the activation of P2X receptor channels permits the influx of both Ca^{2+} and Na^+ ions it is likely that the purinergic Ca^{2+} transients detected in the present study represent the Ca^{2+} component of the EJP. Consistent with this hypothesis is the finding that global Ca^{2+} transients, which represent Ca^{2+} influx during an action potential, are significantly inhibited when purinergic Ca^{2+} transients are blocked. This suggests that the activation of purinergic receptors through EJPs is involved in the initiation of VDCC-dependent action potentials and global Ca^{2+} transients.

Two elementary localized Ca^{2+} events in UBSM: purinergic Ca^{2+} transients and Ca^{2+} sparks

UBSM exhibits two distinct, localized, transient, elementary Ca^{2+} events: purinergic Ca^{2+} transients and

Ca^{2+} sparks. Although similar in appearance, the origin, kinetics, and function of these events are quite different. Purinergic Ca^{2+} transients, mediated by external Ca^{2+} influx through purinergic receptors, have significantly larger amplitudes, longer decay times and greater spatial spread than Ca^{2+} sparks mediated by Ca^{2+} efflux through RyRs located on the sarcoplasmic reticulum (Fig. 6). Ca^{2+} sparks are known to have a 'braking' effect on cell excitability by activating large-conductance Ca^{2+}-sensitive K^+ channels in arterial smooth muscle (for review see Jaggar *et al.* 2000), and have a similar role in UBSM (Imaizumi *et al.* 1999; Herrera *et al.* 2001; Heppner *et al.* 2003). Purinergic Ca^{2+} transients may have just the opposite effect. P2X receptors are non-selective cation channels that exhibit nearly equal permeability to Na^+ and Ca^{2+} ions (Schneider *et al.* 1991). Under physiological conditions, Ca^{2+} ions comprise about 6–8% of the cation influx, with the balance comprised mainly of Na^+ (Schneider *et al.* 1991). The activation of a significant number of P2X clusters could trigger sufficient Na^+ and Ca^{2+} entry to depolarize the membrane potential and activate VDCCs. Subsequent activation of VDCCs would contribute the large amounts of Ca^{2+} that underlie the rising phase of action potentials in UBSM and cause contraction (Creed *et al.* 1983; Klockner & Isenberg, 1985; Heppner *et al.* 1997; Hashitani *et al.* 2000, 2001; Herrera *et al.* 2001).

Clinical conditions increase purinergic activity in the urinary bladder

During certain clinical conditions the contribution of purinergic pathways to excitation–contraction coupling in UBSM is altered. During pregnancy in rats, the composition of purinergic receptors beneath varicosities in the urinary bladder is changed. There is a decrease in clusters of $P2X_1$, $P2X_2$, $P2X_3$, and $P2X_5$, and an increase in subtypes $P2X_4$, and $P2X_6$ (Yunaev *et al.* 2000). In normal human UBSM, purinergic pathways appear to play a minor role. Normally, the density of P2X receptors in human urinary bladders is low compared to rodent urinary bladders (Bo & Burnstock, 1995). However, in unstable, symptomatically obstructed urinary bladders, $P2X_1$ receptor subtype expression is significantly increased (for review see Boselli *et al.* 2001), and patients with idiopathic detrusor instability have a significant purinergic component of nerve-mediated contractions that is absent in normal human bladders (O'Reilly *et al.* 2002). This suggests a plasticity of P2X receptor expression that alters urinary bladder function. Our approach provides the means to examine changes in purinergic signalling at the elementary level in UBSM following outlet obstruction.

This study identifies two distinct types of Ca^{2+} signals exhibited in UBSM using confocal miscroscopy combined with fast Ca^{2+} imaging techniques: global Ca^{2+} flashes and novel, smaller, localized purinergic Ca^{2+} transients. The global Ca^{2+} flashes represent Ca^{2+} influx during action potentials. The smaller, localized purinergic Ca^{2+} transients are not RyR-mediated Ca^{2+} sparks, but instead represent Ca^{2+} influx through P2X receptors located on UBSM cells. These localized purinergic Ca^{2+} transients may represent the initial, crucial steps in the nerve-evoked cascade of events that leads to increases in intracellular Ca^{2+} and contraction of UBSM.

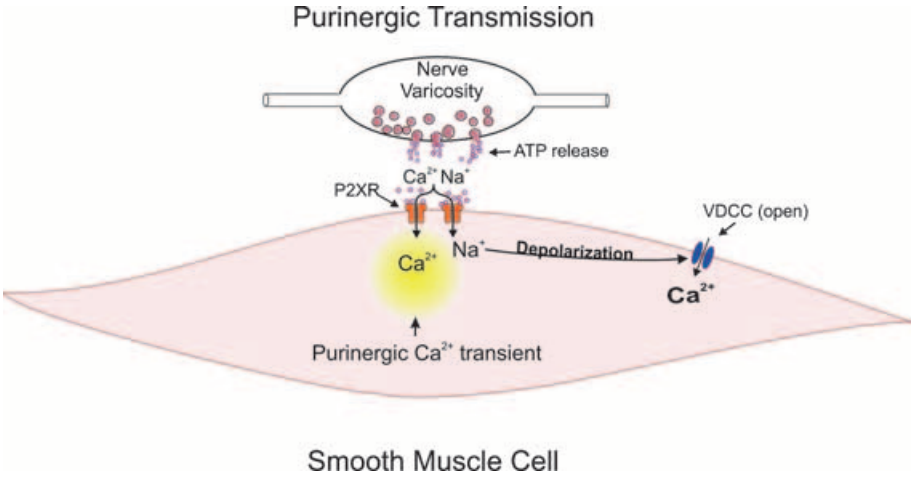

Figure 7. Illustration showing the origin of the purinergic Ca^{2+} transients mediated by P2X receptors
ATP released from parasympathetic nerve varicosities activates P2X receptors located on UBSM. Ca^{2+} influx through the P2X receptors underlies the purinergic Ca^{2+} transients. The membrane potential depolarization arising from Ca^{2+} and Na^+ influx through P2X receptors would open VDCCs allowing significant Ca^{2+} influx into the cell.

References

Birder LA, Ruan HZ, Chopra B, Xiang Z, Barrick S, Buffington CA, Roppolo JR, Ford APDW, de Groat WC & Burnstock G (2004). Atlerations in P2X and P2Y purinergic receptor expression in urinary bladder from normal cats and cats with interstitial cystitis. *Am J Physiol Renal Physiol* **287**, F1084–F1091.

Bo X & Burnstock G (1995). Characterization and autoradiographic localization of [^{3}H]α,β-methylene adenosine 5′-triphosphate binding sites in human urinary bladder. *Br J Urol* **76**, 297–302.

Boselli C, Govoni S, Condino AM & D'Agostino G (2001). Bladder instability: a re-appraisal of classical experimental approaches and development of new therapeutic strategies. *J Autonomic Pharmacol* **21**, 219–229.

Brain KL, Cuprian AM, Williams DJ & Cunnane TC (2003). The sources and sequestration of Ca^{2+} contributing to neuroeffector Ca^{2+} transients in the mouse vas deferens. *J Physiol* **553**, 627–635.

Brain KL, Jackson VM, Trout SJ & Cunnane TC (2002). Intermittent ATP release from nerve terminals elicits focal smooth muscle Ca^{2+} transients in mouse vas deferens. *J Physiol 541* **3**, 849–862.

Bramich NJ & Brading AF (1996). Electrical properties of smooth muscle in the guinea-pig urinary bladder. *J Physiol* **492**, 185–198.

Caulfield MP (1993). Muscarinic receptors—characterization, coupling and function. *Pharmacol Ther* **58**, 319–379.

Creed KE, Ishikawa S & Ito Y (1983). Electrical and mechanical activity recorded from rabbit urinary bladder in response to nerve stimulation. *J Physiol* **338**, 149–164.

Dowdall MJ, Boyne AF & Whittaker VP (1974). Adenosine triphosphate; a constituent of cholinergic synaptic vesicles. *Biochem J* **140**, 1–12.

Drake MJ, Gardner BP & Brading AF (2003). Innervation of the detrusor muscle bundle in neurogenic detrusor overactivity. *BJU Int* **91**, 702–710.

Dutton J, Hansen MA, Balcar VJ, Barden JA & Bennett MR (1999). Development of P2X receptor clusters on smooth muscle cells in relation to nerve varicosities in the rat urinary bladder. *J Neurocytol* **28**, 4–16.

Elneil S, Skepper JN, Kidd EJ, Williamson JG & Ferguson DR (2001). Distribution of $P2X_1$ and $P2X_3$ receptors in the rat and human urinary bladder. *Pharmacol* **63**, 120–128.

Evans RJ, Lewis C, Virginio C, Lundstrom K, Buell G, Surprenant A & North RA (1996). Ionic permeability of, and divalent cation effects on, two ATP-gated cation channels (P2X receptors) expressed in mammalian cells. *J Physiol* **497**, 413–422.

Foster CD, Fujii K, Kingdon J & Brading AF (1989). The effect of cromakalim on the smooth muscle of the guinea-pig urinary bladder. *Br J Pharmacol* **99**, 281–291.

Gabella G (1995). The structural relation between nerve fibres and muscle cells in the urinary bladder of the rat. *J Neurocytol* **24**, 159–187.

Gabella G (1999). Structure of the intramural nerves of the rat bladder. *J Neurocytol* **28**, 615–637.

Gabella G & Davis C (1998). Distribution of afferent axons in the bladder of rats. *J Neurocytol* **27**, 141–155.

Gitterman DP & Evans RJ (2001). Nerve evoked P2X receptor contractions of rat mesenteric arteries; dependence on vessel size and lack of role of L-type calcium channels and calcium induced calcium release. *Br J Pharmacol* **132**, 1201–1208.

Hansen MA, Balcar VJ, Barden JA & Bennett MR (1998). The distribution of single $P2X_1$-receptor clusters on smooth muscle cells in relation to nerve varicosities in the rat urinary bladder. *J Neurocytol* **27**, 529–539.

Hashitani H & Brading AF (2003*a*). Electrical properties of detrusor smooth muscles from the pig and human urinary bladder. *Br J Pharmacol* **140**, 146–158.

Hashitani H & Brading AF (2003*b*). Ionic basis for the regulation of spontaneous excitation in detrusor smooth muscle cells of the guinea-pig urinary bladder. *Br J Pharmacol* **140**, 159–169.

Hashitani H, Brading AF & Suzuki H (2004*a*). Correlation between spontaneous electrical, calcium and mechanical activity in detrusor smooth muscle of the guinea-pig bladder. *Br J Pharmacol* **141**, 183–193.

Hashitani H, Bramich NJ & Hirst GDS (2000). Mechanisms of excitatory neuromuscular transmission in the guinea-pig urinary bladder. *J Physiol 524* **2**, 565–579.

Hashitani H, Fukuta H, Takano H, Klemm MF & Suzuki H (2001). Origin and propagation of spontaneous excitation in smooth muscle of the guinea-pig urinary bladder. *J Physiol 530* **2**, 273–286.

Hashitani H, Yanai Y & Suzuki H (2004*b*). Role of interstitial cells and gap junctions in the transmission of spontaneous Ca signals in detrusor smooth muscles of the guinea-pig urinary bladder. *J Physiol* **559**, 567–581.

Hegde SS & Eglen RM (1999). Muscarinic receptor subtypes modulating smooth muscle contractility in the urinary bladder. *Life Sci* **64**, 419–428.

Heppner TJ, Bonev AD & Nelson MT (1997). Ca^{2+}-activated K^+ channels regulate the repolarization of the action potential in urinary bladder smooth muscle. *Am J Physiol Cell Physiol* **273**, C110–C117.

Heppner TJ, Herrera GM, Bonev AD, Hill-Eubanks D & Nelson MT (2003). Ca^{2+} sparks and K_{Ca} channels: Novel mechanisms to relax urinary bladder smooth muscle. In *Bladder Disease Research Concepts and Clinical Applications*, ed. Atala A & Slade D, pp. 347–357. Kluwer Academic/Plenum Publishers, New York.

Herrera GM, Heppner TJ & Nelson MT (2000). Regulation of urinary bladder smooth muscle contractions by ryanodine receptors and BK and SK channels. *Am J Physiol Regul Integr Comp Physiol* **279**, R60–R68.

Herrera GM, Heppner TJ & Nelson MT (2001). Voltage dependence of the coupling of Ca^{2+} sparks to BK_{Ca} channels in urinary bladder smooth muscle. *Am J Physiol Cell Physiol* **280**, C481–C490.

Herrera GM & Nelson MT (2002). Differential regulation of SK and BK channels by Ca^{2+} signals from Ca^{2+} channels and ryanodine receptors in guinea-pig urinary bladder myocytes. *J Physiol* **541**, 483–492.

Hoyle CH & Burnstock G (1993). Postganglionic efferent transmission in the bladder and urethra. In *Nervous Control of the Urogential System*, ed. Maggi CA, pp. 349–381. Chur, Switzerland: Harwood Academic Publishers.

Iino M, Kasai H & Yamazawa T (1994). Visualization of neural control of intracellular Ca^{2+} concentration in single vascular smooth muscle cells in situ. *EMBO J* **13**, 5026–5031.

Iino M, Yamazawa T, Miyashita Y, Endo M & Kasai H (1993). Critical intracellular Ca^{2+} concentration for all-or-none Ca^{2+} spiking in single smooth muscle cells. *EMBO J* **13**, 5287–5291.

Imaizumi Y, Ohi H, Yamamura H, Ohya S, Muraki K & Watanabe M (1999). Ca^{2+} spark as a regulator of ion channel activity. *Japan J Pharmacol* **80**, 1–8.

Isenberg G, Ganitkevich VYa & Schneider P (1992). Ca^{2+} influx through voltage- and purinoceptor-operated channels estimated from $[Ca^{2+}]$c signals (myocytes from guinea-pig urinary bladder). *Adv Exp Med Biol* **311**, 369–371.

Jaggar JH & Nelson MT (2000). Differential regulation of Ca^{2+} sparks and Ca^{2+} waves by UTP in rat cerebral artery smooth muscle cells. *Am J Physiol Cell Physiol* **279**, C1528–C1589.

Jaggar JH, Porter VA, Lederer WJ & Nelson MT (2000). Calcium sparks in smooth muscle. *Am J Physiol Cell Physiol* **278**, C235–C256.

Kasakov L & Burnstock G (1982). The use of the slowly degradable analog, α,β-methylene ATP, to produce desensitization of the P_2-purinoceptor; effect on non-adrenergic, non-cholinergic responses of the guinea-pig urinary bladder. *Eur J Pharmacol* **86**, 291–294.

Khakh BS, Burnstock G, Kennedy C, King BF, North RA, Seguela P, Voigt M & Humphrey PPA (2001). International Union of Pharmacology. XXIV. Current status of the nomenclature and properties of P2X receptors and their subunits. *Pharmacol Rev* **53**, 107–118.

Klockner U & Isenberg G (1985). Action potentials and net membrane currents of isolated smooth muscle cells (urinary bladder of the guinea-pig). *Pflugers Arch* **405**, 329–339.

Kotlikoff MI, Herrera G & Nelson MT (1999). Calcium permeant ion channels in smooth muscle. *Rev Physiol Biochem Pharmacol* **134**, 147–199.

Lamont C, Vainorius E & Wier WG (2003). Purinergic and adrenergic Ca^{2+} transients during neurogenic contractions of rat mesenteric small arteries. *J Physiol* **549**, 801–808.

Lamont C & Wier WG (2002). Evoked and spontaneous purinergic junctional Ca^{2+} transients (jCaTs) in rat small arteries. *Circ Res* **91**, 454–456.

Lee HY, Bardini M & Burnstock G (2000). Distribution of P2X receptors in the urinary bladder and the ureter of the rat. *J Urol* **163**, 2002–2007.

Mostwin JL (1986). The action potential of guinea pig bladder smooth muscle. *J Urol* **135**, 1299–1303.

Nelson MT, Cheng H, Rubart M, Santana LF, Bonev AD, Knot HJ & Lederer WJ (1995). Relaxation of arterial smooth muscle by calcium sparks. *Science* **270**, 633–637.

Ohi Y, Yamamura H, Nagano N, Ohya S, Muraki K, Watanabe M & Imaizumi Y (2001). Local Ca^{2+} transients and distribution of BK channels and ryanodine receptors in smooth muscle cells of guinea-pig vas deferens and urinary bladder. *J Physiol* **534**, 313–326.

O'Reilly BA, Kosaka AH, Knight GF, Chang TK, Ford AP, Rymer JM, Popert R, Burnstock G & McMahon SB (2002). P2X receptors and their role in female idiopathic detrusor instability. *J Urol* **167**, 157–164.

Perez GJ, Bonev AD, Patlak JB & Nelson MT (1999). Functional coupling of ryanodine receptors to K_{Ca} channels in smooth muscle cells from rat cerebral arteries. *J Gen Physiol* **113**, 229–238.

Schneider P, Hopp HH & Isenberg G (1991). Ca^{2+} influx through ATP-gated channels increments $[Ca^{2+}]_i$ inactivates I_{Ca} in myocytes from guinea-pig urinary bladder. *J Physiol* **440**, 479–496.

Silinsky EM & Redman RS (1996). Synchronous release of ATP and neurotransmitter within milliseconds of a motor nerve impulse in the frog. *J Physiol* **492**, 815–822.

Theobald RJ Jr & de Groat WD (1989). The effects of purine nucleotides on transmission in vesical parasympathetic ganglia of the cat. *J Autonom Pharmacol* **9**, 167–181.

Vial C & Evans RJ (2000). P2X receptor expression in mouse urinary bladder and the requirement of $P2X_1$ receptors for functional P2X receptor reponses in the mouse urinary bladder smooth muscle. *Br J Pharmacol* **131**, 1489–1495.

Wellman GC, Cartin L, Eckman DM, Stevenson AS, Saundry CM, Lederer WJ & Nelson MT (2001). Membrane depolarization, elevated Ca^{2+} entry, and gene expression in cerebral arteries of hypertensive rats. *Am J Physiol Heart Circ Physiol* **281**, H2559–H2567.

Yunaev MA, Barden JA & Bennett MR (2000). Changes in the distribution of different subtypes of P2X receptor clusters on smooth muscle cells in relation to nerve varicosities in the pregnant rat urinary bladder. *J Neurocytol* **29**, 99–108.

Acknowledgements

This study was supported in part by grants from the NIH to M. T. Nelson (DK53832 and DK065947). We would like to thank Drs David Hill-Eubanks, Jessica Filosa, Stephen Straub and Kevin Thorneloe for critically reading this manuscript and providing useful suggestions.

Supplementary material

The online version of this paper can be accessed at:
DOI: 10.1113/jphysiol.2004.077826
http://jp.physoc.org/cgi/content/full/jphysiol.2004.077826/DC1
and contains supplementary material consisting of a movie clip from Fig. 3 showing purinergic Ca^{2+} transients in urinary bladder smooth muscle evoked by field stimulation (1 Hz). Notice that numerous purinergic Ca^{2+} transients occurr in response to each stimulus.
This material can also be found at:
http://www.blackwellpublishing.com/products/journals/suppmat/tjp/tjp740/tjp740sm.htm